RSC Advances

ROYAL SOCIETY OF CHEMISTRY

www.rsc.org/advances

RSC Advances

COMMUNICATION

CL-20 hosted in graphene foam as high energy materials with low sensitivity

Received 00th January 20xx,
Accepted 00th January 20xx

DOI: 10.1039/x0xx00000x

www.rsc.org/

Zhimin Li,[a] Yu Wang,[b] Yanqiang Zhang,*[a] Long Liu[a] and Suojiang Zhang*[a,b]

CL-20/graphene foam (GF) with a guest/host architecture was obtained by in situ crystallization of CL-20 in GF. With high detonation performance (44.1 GPa, 9687 m s^{-1}), the CL-20/GF composite (98/2, w/w) is much less sensitive (IS: 4.5 J, FS: 252 N, ES: 0.72 J) than CL-20 (IS: 2.0 J, FS: 108 N, ES: 0.13 J).

Energetic materials are widely used in both military and civilian fields, including propellants, explosives and pyrotechnics.[1-3] In pursuit of higher chemical potential energy, many new energetic compounds have been steadily synthesized.[4-9] Unfortunately, few of these compounds are proven viable for explosive applications because of thermal or/and mechanical stabilities. The conventional nitramines 1,3,5-trinitroperhydro-1,3,5-triazine (RDX) and octahydro-1,3,5,7-tetranitro-1,3,5,7-tetrazocine (HMX) remain the commonly used explosives.[10-12] Currently, 2,4,6,8,10,12-hexanitro-2,4,6,8,10,12-hexaazaisowurtzitane (CL-20) with high density (about 2.0 g cm^{-3}) and superior performance (44.8 GPa and 9762 m s^{-1}, about 14% higher than HMX) is regarded as one of the most promising compounds to replace RDX and HMX.[13-15] However, the high sensitivities of CL-20 (2.0 J and 108 N) block its widespread applications. Developing efficient methods to desensitize CL-20 is critically necessary, and has become a challenging task.

Some works have been conducted to lower CL-20's sensitivities.[16-21] Besides controlling the morphology and granularity, doping less sensitive components has been proved very efficient to desensitize CL-20. For example, crystallization of CL-20 with trinitrotoluene (TNT) can form their co-crystal in 1:1 molar ratio.[22] Though the CL-20/TNT cocrystals exhibit lower impact sensitivity, their explosive power is reduced too much for TNT weights as 34 wt%. Another co-crystal of CL-20/HMX in 2:1 molar ratio was obtained by Matzger's group, and became a promising replacement of HMX.[23] Interestingly, graphene possessing many desired properties (ultralow mass density, good lubrication, superior electrical and thermal conductivities) has been used as the component to desensitize energetic materials.[24-26] Previously, we used 2D graphene nanoplates (1 wt%) to reduce the electrostatic hazards of primary explosives, resulting an excellent anti-electrostatic graphene nanoplatelet/lead styphnate composite for igniter applications.[27] Compared with 2D graphene, the 3D graphene foam (GF) possesses continuously interconnected macroporous structure which is an ideal scaffold with synergistic effects on the integration with other materials.[28-31] Therefore, loading CL-20 in 3D GF could be a convenient way to combine the energy and sensitivities of energetic materials, which has not reported yet.

In this study, CL-20 was investigated to host in GF, and the resulting CL-20/GF composite was characterized in details. Thermal decomposition mechanism, energetic properties and sensitivities of CL-20/GF were studied comparing with pure CL-20. Except for a low sensitive high energetic CL-20/GF composite was obtained, the new use of GF as a substrate of energetic materials was introduced in this work, and the guest/host architecture of high energetic compounds in porous materials may be an effective way for the balance of high energy and low sensitivity of energetic materials.

The raw CL-20 was provided from China Academy of Engineering Physics, and purified by recrystallization with a solvent-nonsolvent method. GF was obtained via a CVD method according to previous literatures,[31] using nickel foam as substrate and catalyst, and ethanol as the carbon source for graphene growth under atmospheric pressure. After GF was immersed into a solution of CL-20 in ethyl acetate, CL-20 crystals were obtained *in situ* into GF by slow evaporation of ethyl acetate in room temperature. The fabrication process for CL-20/GF composite is depicted in Fig. 1. Details for the preparation of GF, CL-20, and CL-20/GF can be found in Section S2.

[a] Beijing Key Laboratory of Ionic Liquids Clean Process, Key Laboratory of Green Process and Engineering, Institute of Process Engineering, Chinese Academy of Sciences, Beijing 100190, P. R. China. Email: yqzhang@ipe.ac.cn, sjzhang@ipe.ac.cn

[b] State Key Laboratory of Multiphase Complex Systems, Institute of Process Engineering, Chinese Academy of Sciences, Beijing 100190, P. R. China.

† Electronic Supplementary Information (ESI) available: [details of any supplementary information available should be included here]. See DOI: 10.1039/x0xx00000x

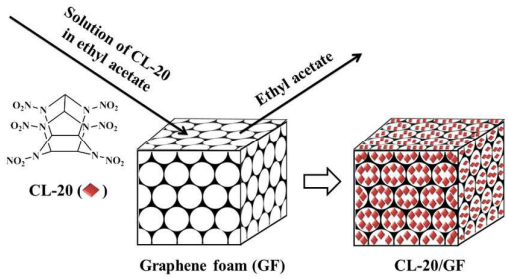

Fig. 1 Schematic illustration of the fabrication of CL-20/GF.

The obtained CL-20/GF, as well as CL-20 and GF, was characterized by using Raman spectroscopy, X-ray diffraction (XRD) and field-emission scanning electron microscopy (FE-SEM) with an energy dispersive spectrometer. In the Raman spectra (Fig. 2), there are two characteristic peaks for GF as 1579 (G band) and 2722 cm^{-1} (2D band), and no appreciable D band (1350 cm^{-1}) indicates the high quality of GF.[29] The Raman shifts featured in both CL-20 and GF were found in the spectrum of the as-prepared CL-20/GF composite. Compared with the Raman spectrum of CL-20, the peaks at 1585 and 2708 cm^{-1} are the corresponding G and 2D bands of CL-20/GF composite. The XRD patterns of CL-20, GF and CL-20/GF were shown in Fig. 2b. GF displays two diffraction peaks at 26.5 and 54.6°, attributed to the (002) and (004) reflections of graphitic carbon, respectively (JCPDS card no. 75–1621).[31] The diffraction peaks of CL-20/GF are mainly resulting from CL-20, with two additional peaks at 26.5 and 54.6° showing the presence of GF.

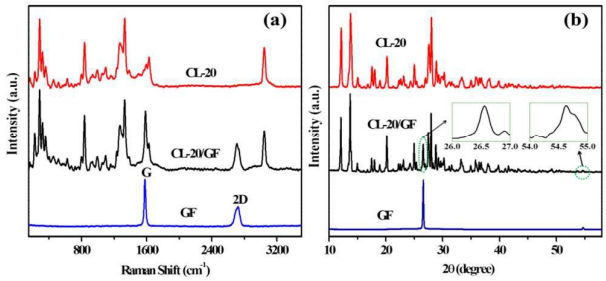

Fig. 2 (a) Raman spectra and (b) XRD patterns of CL-20/GF compared with CL-20 and GF.

The morphologies of CL-20, GF, and CL-20/GF were studied by using SEM (Fig. 3). The bulky CL-20 crystals are shown in Fig. 3a. The interconnected and macroporous three-dimensional graphene reticular architecture of GF was confirmed in Fig. 3b and 3c at low- and high-magnification, respectively. Fig. 3d-f shows the typical morphologies of CL-20/GF at different magnifications. As can be seen, CL-20 crystals are well distributed in the 3D GF frameworks. Induced by the presence of GF, the crystals of CL-20 closely grew on GF surface one by one, layer upon layer. A low-magnification SEM image of CL-20/GF can be seen in Fig. 3g, and the corresponding elemental mapping images for C, N and O are shown in Fig. 3h, 3i and 3j, respectively. The consistent distribution of C, N and O further confirmed the good combination of CL-20 and GF moieties in the composite. The contents of N and O obtained by energy dispersive spectroscopy (EDS) are 32.35 % and 38.95 %, and the ratio (0.83) is approximate to that of CL-20 (0.87). The C content of CL-20/GF (28.70 %) is much higher than that of CL-20 (16.45 %) since GF is totally composed of carbon.

Thermal decomposition process of CL-20/GF composite and CL-20 were contrastively investigated by applying differential scanning calorimetry (DSC). An advanced decomposition temperature of CL-20/GF can be clearly founded in the DSC curves (Fig. 4). The onset and peak temperatures of CL-20/GF are 214 and 245 °C, which are 16 and 14 °C lower than those of pure CL-20, respectively. The lower decomposition temperatures of CL-20/GF indicate the catalysis effect of GF.

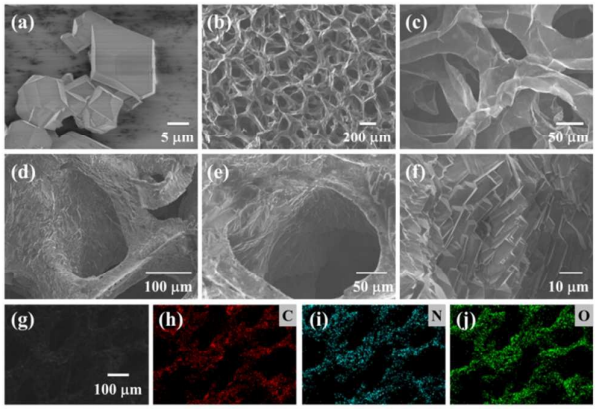

Fig. 3 (a) SEM image of CL-20. (b, c) Low- and high-magnification SEM images of GF. (d-f) SEM images of CL-20 hosted in GF. (g) A low-magnification SEM image of CL-20/GF and the corresponding elemental mapping images for carbon (h), nitrogen (i) and oxygen (j).

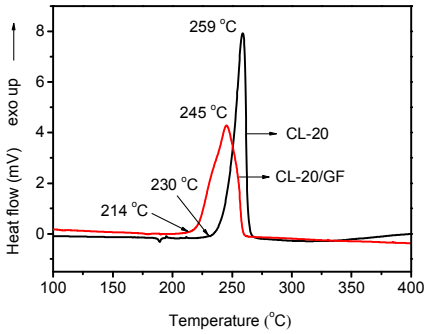

Fig. 4 DSC curves for CL-20/GF and CL-20 (heating rate 10 °C min^{-1}, under N_2 atmosphere).

To further assess the thermal decomposition of CL-20/GF, the kinetic parameters including apparent activation energy (E_a) and pre-exponential factor (A) were calculated by employing Kissinger and Ozawa-Doyle equations which are given in Formula S1.[32-34] Results obtained from the both methods are similar, and in the normal range of kinetic parameters for the thermal decomposition reactions of solid materials.[35] The mean value of E_a for CL-20/GF is 92.0 kJ·mol^{-1} which is much smaller than that of pure CL-20 (169.2 kJ·mol^{-1}). The values of A for CL-20/GF and CL-20 are $10^{6.91}$ and $10^{14.67}$ s^{-1}, respectively. Arrhenius equations of the decomposition process of CL-20/GF and CL-20 can be expressed as: $\ln k = 15.91 - 92.0 \times 10^3 / RT$ and $\ln k = 33.78 - 169.2 \times 10^3 / RT$, respectively. The much reduced E_a and A show the good catalysis effect of GF on the thermal decomposition of CL-20.

The detonation pressure and velocity of CL-20/GF composite were calculated with an EXPLO5(V6.02) program for evaluating its energetic properties.[37] Parameters of GF in the calculations were applied with those of graphite. Various contents (0.5, 1, 2, 3, 4, and 5 wt%) of GF were selected to check the influence of CL-20/GF ratios on detonation properties. As shown in Fig. 5, the detonation pressures and velocities of CL-20/GF were reduced along with the increase of the content of GF, but they are still higher than those of HMX and RDX. On the other hand, as the increase of non-energetic GF, the sensitivities of CL-20/GF composite were lowered gradually.

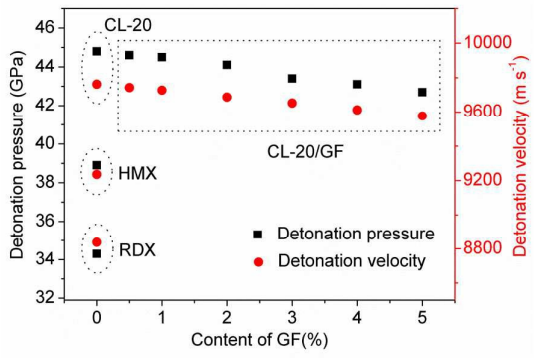

Fig. 5 Detonation performances of CL-20/GF with various content of GF compared with CL-20, HMX and RDX, respectively

With a content of 2 wt% GF, the impact sensitivity, friction sensitivity and electrostatic spark sensitivity of CL-20/GF were tested by employing a standard BAM Fallhammer, a BAM friction tester and a JGY-II tester, respectively. Results of CL-20/GF compared with CL-20, HMX[1] and RDX[1] were listed in Table 1. CL-20/GF exhibits two times less impact and fraction sensitives (4.5 J, 252 N) than CL-20 (2.0 J, 108N). The much reduced mechanical sensitivities of CL-20/GF are supposed from the excellent lubrication and heat conduction of GF, which could reduce the internal folding dislocations and hot spots. The electrostatic spark sensitivity of CL-20/GF was reduced from 0.72 to 0.13 J due to the superior conductivity of GF. Fig. 6 shows a visual comparison of the sensitivities of CL-20/GF, CL-20, HMX and RDX, respectively. Except for the impact sensitivity, CL-20/GF is the most insensitive one.

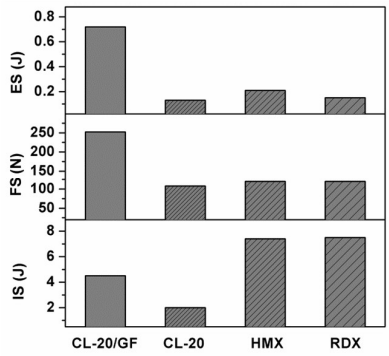

Fig. 6 Sensitivities of CL-20/GF (98/2, w/w) compared with CL-20, HMX and RDX.

Table 1 Detonation properties and sensitivities of CL-20/GF (98/2, w/w) compared with CL-20, HMX and RDX.

	P (GPa)[a]	v_D (m s^{-1})[b]	*IS* (J)[c]	*FS* (N)[d]	*ES (J)*[e]
CL-20/GF	44.1	9687	4.5	252	0.72
CL-20	44.8	9762	2.0	108	0.13
HMX	38.9	9235	7.4[1]	120[1]	0.21[1]
RDX	34.3	8838	7.5[1]	120[1]	0.15[1]

[a] Detonation pressure (calculated with EXPLO5(V6.02)). [b] Detonation velocity (EXPLO5(V6.02)). [c] Impact sensitivity (tested according to standard BAM methods). [d] Friction sensitivity (tested according to standard BAM methods). [e] Electrostatic spark sensitivity (tested by using a JGY-II tester).

In conclusion, CL-20 hosted in GF was prepared by a facile *in situ* recrystallization method. The unique guest-host architecture of CL-20 decorated in GF was characterized by Raman spectroscopy, XRD and SEM. The decreased thermal decomposition temperature and apparent activation energy of CL-20/GF indicate the remarkable catalysis effect of GF on the CL-20 decomposition. CL-20/GF (98/2, w/w) maintains the excellent energetic properties with the detonation and detonation velocity as 44.1 GPa and 9687 m s^{-1}, while its sensitivities (IS: 4.5 J, FS: 252 N, ES: 0.72 J) are much lower than those of CL-20 (IS: 2.0 J, FS: 108 N, ES: 0.13 J) so that the hazard aroused by mechanical and electrostatic stimulates was greatly reduced. With the good combination detonation performance with sensitivities, the as-prepared CL-20/GF composite may be applied as a moiety of secondary explosive or solid rocket propellant for safer applications.

Acknowledgements

The authors gratefully acknowledge the support from the National Natural Science Foundation of China (21376252 and 21406242); Beijing Natural Science Foundation (2154057); The National Defense Science and Technology Innovation Fund of Chinese Academy of Sciences (CXJJ-14-M37 and CXJJ-14-M41) and China Postdoctoral Science Foundation (2015M571128).

Notes and references

1 T. M. Klapötke, *Chemistry of High-Energetic Materials (2 nd Edition)*, Walter de Gruyter GmbH & Co. KG Berlin, 2012.
2 J. P. Agrawal and R. Hodgson, *Organic Chemistry of Explosives*, Wiley, New York, 2007.
3 J. Akhavan, *The Chemistry of Explosives*, Royal Society of Chemistry, Cambridge, 1998.
4 H. X. Gao and J. M. Shreeve, *Chem. Rev.*, 2011, **111**, 7377-7436.
5 T. M. Klapötke, P. C. Schmid, S. Schnell and J. Stierstorfer, *J. Mater. Chem. A*, 2015, **3**, 2658-2668.
6 D. Fischer, T. M. Klapötke and J. Stierstorfer, *Angew. Chem. Int. Ed.*, 2014, **53**, 8172-8175.
7 J. H. Zhang, Q. H. Zhang, T. T. Vo, D. A. Parrish and J. M. Shreeve, *J. Am. Chem. Soc.*, 2015, **137**, 1697-1704.
8 Y. Q. Zhang, D. A. Parrish and J. M. Shreeve, *J. Mater. Chem. A*, 2013, **1**, 585-593.
9 Y. Q. Zhang, D. A. Parrish and J. M. Shreeve, *J. Mater. Chem.*, 2012, **22**, 12659-12665.
10 A. T. Nielsen, A. P. Chafin, S. L. Christian, D. W. Moore, M. P. Nadler, R. A. Nissan, D. J. Vanderah, R. D. Gilardi, C. F. George and J. L. Flippen-Anderson, *Tetrahedron*, 1998, **54**, 11793-11812.

11 B. Risse, F. Schnell and D. Spitzer, *Propellants Explos. Pyrotech.*, 2014, **39**, 397-401.
12 B. Huang, X. F. Hao, H. B. Zhang, Z. J. Yang, Z. G. Ma, H. Z. Li, F. D. Nie and H. Huang, *Ultrason. Sonochem.*, 2014, **21**, 1349-1357.
13 R. L. Simpson, P. A. Urtiew, D. L. Ornellas, G. L. Moody, K. F. J. Scribner and D. M. Hoffman, *Propellants Explos. Pyrotech.*, 1997, **22**, 249-255.
14 A. K. Mandal, C. S. Pant, S. M. Kasar and T. Soman, *J. Energ. Mater.*, 2009, **27**, 231-246.
15 U. R. Nair, R. Sivabalan, G. M. Gore, M. Geetha, S. N. Asthana and H. Singh, *Combust. Explo. Shock*, 2005, **41**, 121-132.
16 J. Shen, W. Shi, J. Wang, B. Gao, Z. Qiao, H. Huang, F. Nie, R. Li, Z. Li, Y. Liu and G. Yang, *Phys. Chem. Chem. Phys.*, 2014, **16**, 23540-23543.
17 D. Spitzer, B. Risse, F. Schnell, V. Pichot, M. Klaumunzer and M. R. Schaefer, *Sci. Rep.*, 2014, **4**, 6575(6501-6506).
18 X. D. Guo, G. Ouyang, J. Liu, Q. Li, L. X. Wang, Z. M. Gu and F. S. Li, *J. Energ. Mater.*, 2015, **33**, 24-33.
19 Y. Bayat, M. Zarandi, M. A. Zarei, R. Soleyman and V. Zeynali, *J. Mol. Liq.*, 2014, **193**, 83-86.
20 D. I. A. Millar, H. E. Maynard-Casely, D. R. Allan, A. S. Cumming, A. R. Lennie, A. J. Mackay, I. D. H. Oswald, C. C. Tang and C. R. Pulham, *CrystEngComm*, 2012, **14**, 3742-3749.
21 J. Liu, H. Ren, Q. J. Jiao and L. Yu, *Integr. Ferroelectr.*, 2014, **152**, 127-136.
22 O. Bolton and A. J. Matzger, *Angew. Chem. Int. Ed.*, 2011, **50**, 8960-8963.
23 O. Bolton, L. R. Simke, P. F. Pagoria and A. J. Matzger, *Cryst. Growth Des.*, 2012, **12**, 4311-4314.
24 L. Yu, H. Ren, X. Y. Guo, X. B. Jiang and Q. J. Jiao, *J. Therm. Anal. Calorim.*, 2014, **117**, 1187-1199.
25 X. Wang, J. Li, Y. Luo and M. Huang, *Sci. Adv. Mater.*, 2014, **6**, 530-537.
26 C. Zhang, X. Cao and B. Xiang, *J. Phys. Chem. C*, 2010, **114**, 22684-22687.
27 Z. M. Li, M. R. Zhou, T. L. Zhang, J. G. Zhang, L. Yang and Z. N. Zhou, *J. Mater. Chem. A*, 2013, **1**, 12710-12714.
28 Z. Chen, W. Ren, L. Gao, B. Liu, S. Pei and H. M. Cheng, *Nat. Mater.*, 2011, **10**, 424-428.
29 H. Y. Yue, S. Huang, J. Chang, C. Heo, F. Yao, S. Adhikari, F. Gunes, L. C. Liu, T. H. Lee, E. S. Oh, B. Li, J. J. Zhang, H. Ta Quang, L. Nguyen Van and Y. H. Lee, *Acs. Nano.*, 2014, **8**, 1639-1646.
30 J. Wang, J. Liu, D. Chao, J. Yan, J. Lin and Z. X. Shen, *Adv. Mater.*, 2014, **26**, 7162-7169.
31 X. C. Dong, H. Xu, X. W. Wang, Y. X. Huang, M. B. Chan-Park, H. Zhang, L. H. Wang, W. Huang and P. Chen, *Acs. Nano.*, 2012, **6**, 3206-3213.
32 H. E. Kissinger, *Anal. Chem.*, 1957, **29**, 1702-1706.
33 T. Ozawa, *Bull. Chem. Soc. Jpn.*, 1965, **38**, 1881-1886.
34 R. Z. Hu, S. L. Gao, F. Q. Zhao, Q. Z. Shi, T. L. Zhang and J. J. Zhang, *Thermal Analysis Kinetics (2 nd Edition)*, Science Press, Beijing, 2008.
35 R. Z. Hu, Z. Q. Yang and Y. J. Liang, *Thermochim. Acta*, 1988, **123**, 135-151.
36 H. X. Gao, F. Q. Zhao, R. Z. Hu, Y. Luo, L. B. Xiao, N. Li, X. N. Ren, X. X. Hao and Q. Pei, *Chinese J. Explos. Propell.*, 2013, **36**, 41-48.
37 M. Sućeska, EXPLO5 6.02, Zagreb, Croatis, 2014.

Table of Content:

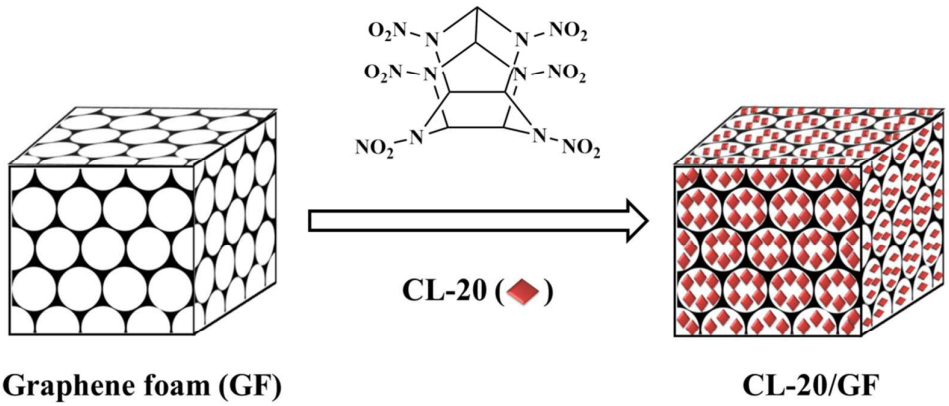

2,4,6,8,10,12-Hexanitro-2,4,6,8,10,12-hexaazaisowurtzitane (CL-20)/graphene foam (GF) composite with a guest-host architecture was prepared as high energy materials with low sensitivity.